Performance Characteristics of a Newly Developed Cost-Effective Cr-Ni Prealloyed Steel Designed to replace Fe-Ni Steels

Nagarjuna Nandivada, David Milligan and Alexander Klekovkin
North American Höganäs
Yoshinobu Takeda, Höganäs Japan
Yang Yu, Höganäs AB, Sweden

ABSTRACT

Many PM applications requiring very good heat treated properties have utilized the FN-020X material system due to the relative economy of the system and ease of use. Recently, however, increases and wide fluctuations in the price of nickel have made the FN material systems less attractive. The FN system has also been challenging to use in applications requiring tight dimensional tolerances due to inconsistencies in dimensions related to negative dimensional change and segregation of admixed nickel. Many of the Cr-based systems introduced in the last few years have lower total alloy cost and excellent properties, but require careful sintering and heat treatment.

The purpose of this paper will be to demonstrate the properties achievable with a new prealloyed Cr-Ni steel (Astaloy CMN) that is suitable for sintering in endogas and for conventional atmosphere heat treatment. The heat treated properties of this new Cr-Ni prealloyed steel equal or exceed the FN-020X system while providing significantly lower total alloying cost. The focus of this paper is to present heat treated properties of test specimens sintered both in 90 $^{v}/_{o}N_2$/10 $^{v}/_{o}H_2$ and Endogas.

INTRODUCTION

In order to expand the Powder Metal (PM) market into new applications, cost effective materials with increased performance are required. Using pre-alloyed powders, higher performance levels can be achieved. With the availability of new powder manufacturing technologies and nitrogen-hydrogen sintering atmospheres the advantages of chromium PM steel can be fully utilized [1]. Chromium PM steels offer the advantages of high performance, lower alloy cost, and good dimensional stability [2]. The less expensive Fe-Cu-C mixes may be attractive at times but have lower dimensional consistency and lower performance.

Common pre-alloying elements used in PM are nickel and molybdenum due to ease of processing. However, these elements have become very costly and are not necessarily the best when it comes to dimensional stability. The raw material costs for Ni and Mo for applications utilizing traditional heat-treated PM materials have seen an astronomical rise in recent years. Figure 1 shows market price development for these elements compared to chromium since 2002. This has reduced levels of profitability within the entire value chain to low levels and even threatens the competitiveness of specific

PM applications to competing metal forming techniques. Consequently urgent demands have arisen from End Users, System Suppliers and Component Producers alike, for innovative cost effective solutions.

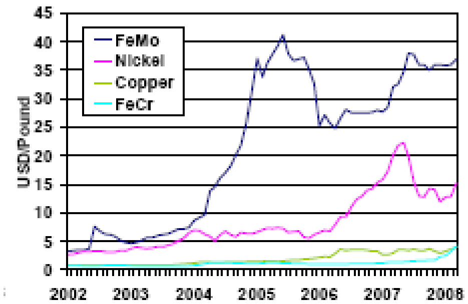

Figure 1. Alloying element cost evolution since 2002 [3].

This paper will demonstrate the heat treated properties of a new prealloyed material Astaloy CMN developed at North American Höganäs. Astaloy CMN is a cost effective alloy for heat-treatment which uses a combination effect of lean Cr and Ni with small amounts of Mo and Mn.

EXPERIMENTAL PROCEDURE

Powders and Materials

The material used in the experiments is based on the new pre-alloyed Cr-Mo-Ni-Mn steel powder - Astaloy CMN. The chemical composition of this powder is shown in Table I below.

Table I. Chemical composition of the base powder used

Base Powder	Cr (%)	Mo (%)	Ni (%)	Mn (%)	Fe (%)
Astaloy CMN	0.56	0.11	0.55	0.10	Balance

Premixes based on this powder with the compositions listed in Table II were prepared. Asbury 1651 graphite was used in all cases and the lubricant used was 0.6% Kenolube from Höganäs AB.

Table II. Materials compositions

Designation	Base Powder	Graphite, $^{w}/_{0}$
A	Astaloy CMN	0.2
B	Astaloy CMN	0.6

Sample preparation

Transverse Rupture Strength (TRS) and Izod impact energy bars were compacted from each mix using a Gasbarre Mechanical 100 ton press (Figure 2). Conventional compaction was used in order to obtain desired density of 7.10 g/cm³. To achieve 7.30 g/cm³ the double press – double sinter technique was used: first press – 7.10 g/cm³ (593 MPa (43 tsi)); first sinter – 787°C (1420°F) for 15 minutes; second press – 7.30 g/cm³ (662 MPa (48 tsi)); second sinter – 1121°C (2050°F). The specimens for tensile strength were machined from impact energy bars to get round test bars according to MPIF 10 standard (Figure 2). The compressibility curve for the Material B is shown in Figure 2.

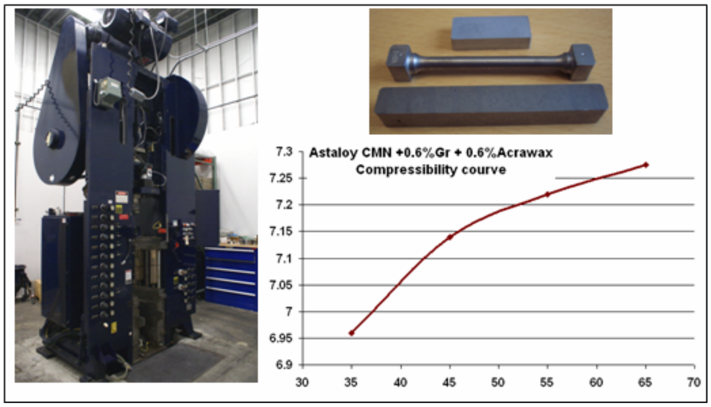

Figure 2. 100-ton press, test specimens and compressibility curve.

Sintering

The test specimens were sintered with normal cooling rates (Table III) in an Abbott 6” mesh belt furnace with conventional nitrogen-hydrogen atmosphere as well as in endogas (external production furnace) with the conditions described in Table III below.

Table III. Sintering conditions

Description	N_2/H_2 (N)	Endogas (E)
Furnace type	Mesh belt	Mesh belt
Temperature, °C (°F)	1120 (2050)	1110 (2030)
Atmosphere	$90N_2$ / $10H_2$	Endogas, +30°F Dewpoint
Time at temperature	30 min	25 min
Cooling rate, °C/s (°F/s)	0.5 (1.0)	0.5 (1.0)

Heat Treatment

Heat treatment was performed at Pennsylvania Industrial Heat Treaters (St. Mary’s, Pennsylvania) based on parameters described in Table IV.

Table IV. Heat treating parameters.

Parameters	Material A	Material B
	Case hardening	Through hardening
Type	Batch	Batch
Temperature	899°C (1650°F)	843°C (1625°F)
Carbon potential	0.8 %C	0.6 %C
Soak time	30 min	90 min
Atmosphere	Endothermic gas	
Quenching	Oil 60°C (140°F)	
Tempering	177°C (350°F) for 1 hour	

Testing
Carbon and oxygen contents were determined for Materials A and B after sintering using Leco infrared combustion analyzers according to ASTM E 1019-02. Dimensional change was tested using TRS bars after each type of sintering and heat treatment according to MPIF standard 44. Apparent hardness, transverse rupture strength, impact energy and tensile tests were evaluated for both materials as sintered and as heat treated for both densities, sintering conditions and heat treatments per MPIF standards 43, 44, 40 and 10. Determination of microindentation hardness and effective case depth were performed according to MPIF standards 51 and 52.

RESULTS AND DISCUSSION

Density
Table V shows densities obtained after sintering and heat-treatment of Materials A and B.

Table V. Density of Materials A and B

Material		A (Astaloy CMN + 0.2%C)				B (Astaloy CMN + 0.6%C)			
Green density	Specimen	A^{N}	$A^{N/CQT}$	A^{E}	$A^{E/CQT}$	B^{N}	$B^{N/QT}$	B^{E}	$B^{E/QT}$
7.10 g/cm³	TRS	7.14	7.11	7.11	7.09	7.13	7.11	7.09	7.11
	IE	7.14	7.13	7.12	7.10	7.10	7.09	7.08	7.08
7.30 g/cm³	TRS	7.30	7.28	7.28	7.28	7.29	7.29	7.27	7.28
	IE	7.33	7.32	7.28	7.27	7.32	7.30	7.29	7.29

A^{N} and B^{N} – $90N_2/10H_2$ sintered and A^{E} and B^{E} – Endogas sintered;
$A^{N/CQT}$ $A^{E/CQT}$ – Case Carburized and $B^{N/QT}$ $B^{E/QT}$ – Through Hardened.

Sintered Carbon and Oxygen
Carbon and oxygen contents for both materials are shown in Table VI after sintering and heat-treatment. The carbon content in the case was estimated metallographically.

Table VI. Carbon and Oxygen after sintering and heat-treatment

Density	Material A (Astaloy CMN + 0.2%C)			Material B (Astaloy CMN + 0.6%C)		
	Procedure	C (%)	O_2 (%)	Procedure	C (%)	O_2 (%)
7.10 g/cm³	A^{N}	0.14	0.02	B^{N}	0.52	0.02
	$A^{N/CQT}$ (case)	0.6	-	$B^{N/QT}$	0.65	-
	A^{E}	0.33	0.10	B^{E}	0.53	0.07
	$A^{E/CQT}$ (case)	0.6	-	$B^{E/QT}$	0.64	-
7.30 g/cm³	A^{N}	0.15	0.02	B^{N}	0.52	0.02
	$A^{N/CQT}$ (case)	0.6	-	$B^{N/QT}$	0.63	-
	A^{E}	0.28	0.11	B^{E}	0.54	0.07
	$A^{E/CQT}$ (case)	0.6	-	$B^{E/QT}$	0.64	-

Material A sintered in endogas was higher in carbon due to carbon pick up during the sintering process. The oxygen content in both materials after sintering in endogas was slightly higher compared to nitrogen-hydrogen atmosphere but acceptable.

Dimensional Change

Dimensional change (DC) during sintering and heat treatment was evaluated from die to as-sintered size. Figure 3 shows the influence of density and sintering.

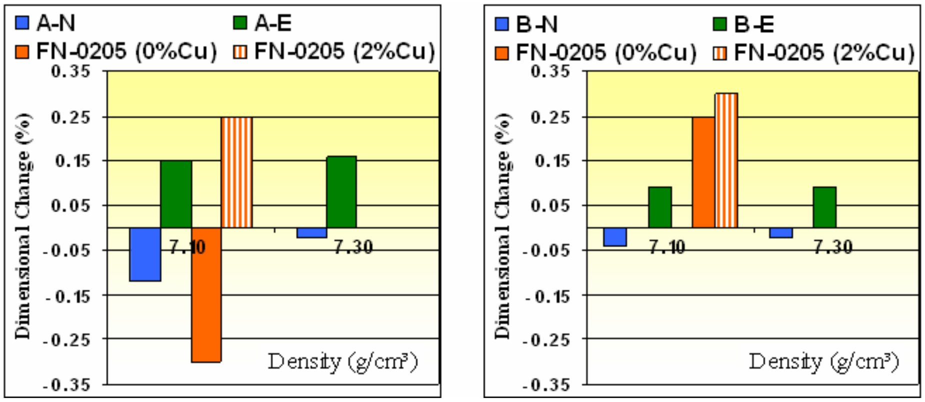

Figure 3. Dimensional change of sintered Materials A and B compared to FN-0205-HT.

Sintering in nitrogen-hydrogen atmosphere showed slight shrinkage while endo gas showed slight growth in dimensions. Both materials showed much lower dimensional change than FN-0205-HT steels. Material A and Material B showed better consistency of dimensional change with respect to density.

Apparent Hardness

Figure 4 shows apparent hardness achieved after sintering and heat treatment.
This material shows normal trends for apparent hardness, i.e. hardness increased with density and increased with higher carbon content.

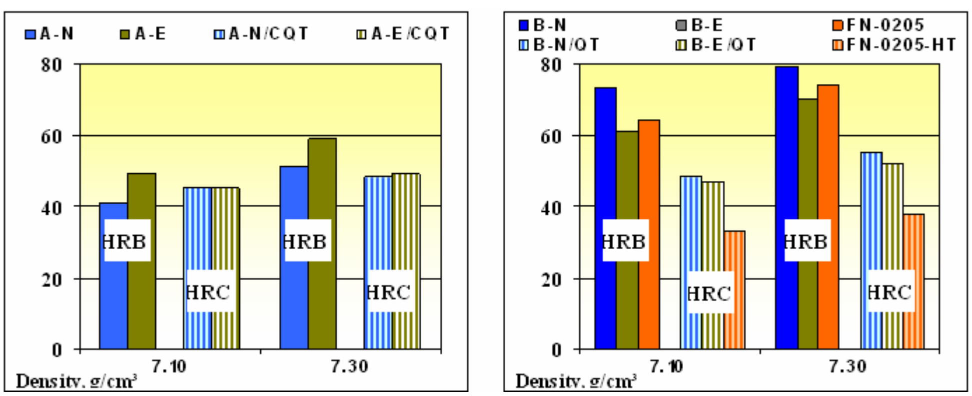

Figure 4. Rockwell Apparent hardness of heat treated Materials A and B compared to FN-0205-HT.

Through hardened Material B obtained apparent hardness much higher than similarly processed FN-0205-HT. The high apparent hardness is due to the net effect of the combination of Cr and Ni.

Microindentation hardness

Material A: Astaloy CMN + 0.2% Graphite.

The microindentation hardness profile of case-carburized Material A measured from the surface is reported in Figure 5.

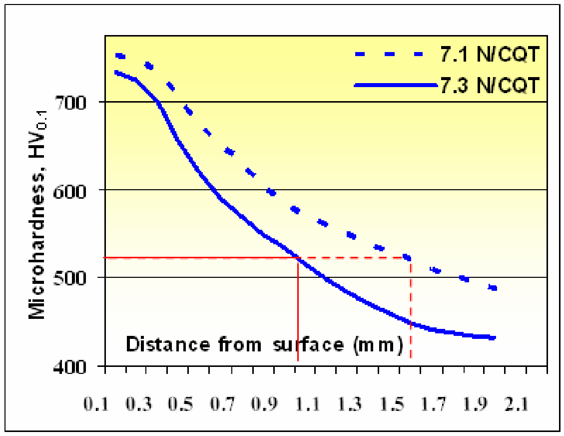

Figure 5. Microindentation hardness of carburized case hardened Material A.

The effective case depth at a minimum of 515 $HV_{0.1}$ (equivalent to ~50 HRC) obtained was about 1.6 mm (0.0629") in case of density 7.10 g/cm³ and case depth about 1.0 mm (0.0393) for 7.30 g/cm³ for the conditions used (Table IV).

Material B: Astaloy CMN + 0.6% Graphite

Microindentation hardness of Material B after through hardening is reported in Table VII.

Table VII. Microindentation hardness of through hardened Material B

Designation	g/cm³	$B^{N/QT}$	$B^{E/QT}$
Microindentation hardness ($HV_{0.1}$)	7.10	748	724
	7.30	786	790

Microindentation hardnesses up to 790 $HV_{0.1}$ were achieved at a depth of 0.1 mm (0.0039") from the surface, which is equivalent to approximately 64 HRC.

Transverse Rupture Strength
Figure 6 shows the transverse rupture strengths of sintered and through hardened Material B at different densities comparing to FN-0205-HT steel.

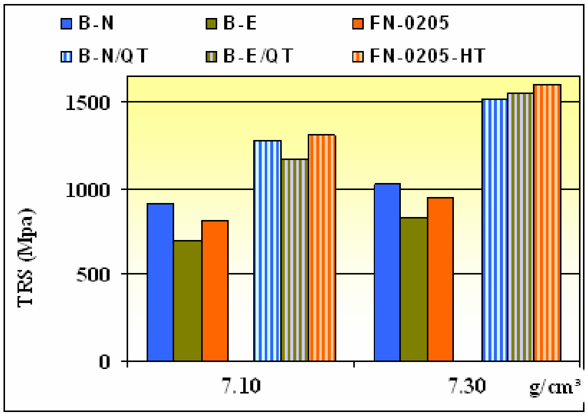

Figure 6. Transverse rupture strengths of sintered and through hardened Material B at different densities comparing to FN-0205-HT.

As expected the transverse rupture strength increased with increased density. After heat-treatment the transverse rupture strength increased up to 50%. The result shows Astaloy CMN compares well to the TRS of FN0205-HT material.

Impact Energy
Unnotched impact energy of Material B after sintering and heat treatment is shown in Figure 7.
The un-notched Charpy impact energy increases with increase in density. On the other hand, the heat-treatment decreases the impact energy at all density levels which is an effect of the increased amount of martensite in the microstructure. As can be seen after heat-treatment impact energy is very similar to FN-0205-HT steel.

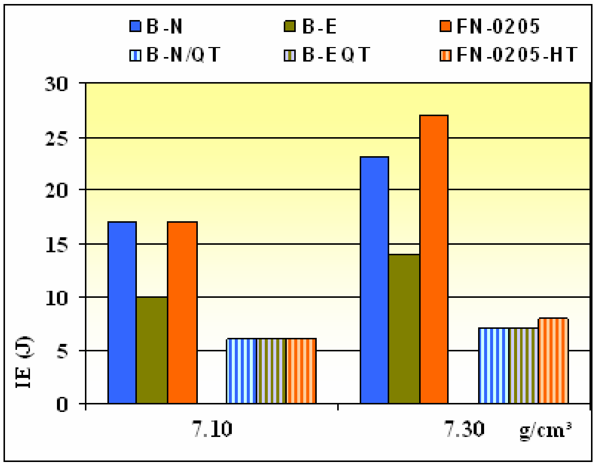

Figure 7. Impact Energy of Material B after different sintering and heat treatment comparing to FN-0205-HT steel.

Ultimate Tensile Strength

Tensile Strength of Material B after sintering and heat treatment compared to FN-0205-HT steel is shown in Figure 8.

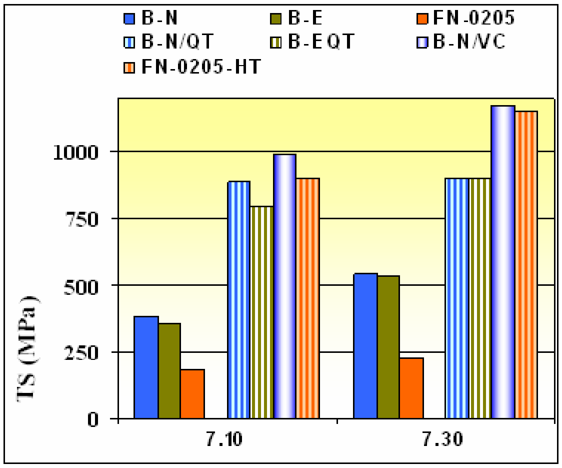

Figure 8. Tensile Strength of Material B after different sintering and heat treatment comparing to FN-0205-HT steel.

By through hardening the tensile strength is increased about 70% and is close to FN-0205HT at 7.10 g/cm³. This is a result of achieving a martensitic microstructure. One trial of vacuum carburization also was performed at Hayes Heat Treating (Rhode Island) and even higher tensile strength (up to two times comparing to as sintered) was obtained. After vacuum carburization tensile strength even exceeds FN-0205-HT steel requirements.

Microstructure after sintering

The etched microstructures of Material A (Astaloy CMN + 0.2% graphite mix) and Material B (Astaloy CMN + 0.6% graphite mix) obtained after sintering in nitrogen-hydrogen atmosphere are shown in Figure 9 below.

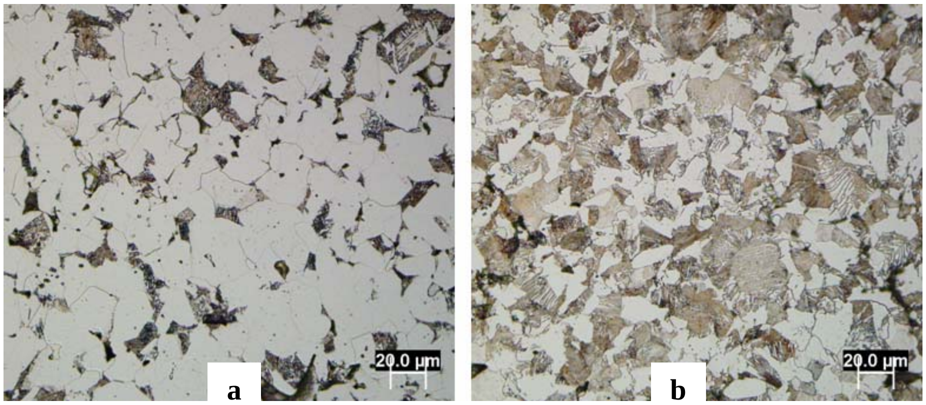

Figure 9. Sintered microstructures: ***a*** – Material A; ***b*** – Material B.

The microstructure of Material A with 0.14 % C mostly consists of ferrite and small amount of pearlite. The microstructure of Material B with 0.52 %C after sintering mostly consists of pearlite, ferrite and some upper bainite.

Microstructure after heat treatment

The microstructures of Material A at density 7.10 g/cm³ after sintering in nitrogen-hydrogen atmosphere and heat treatment are shown in Figure 10. As can be seeing, after case hardening Material A obtained martensitic microstructures in the case (Figure 10a) and mostly bainite-pearlite with some martensite in the center (Figure 10b).

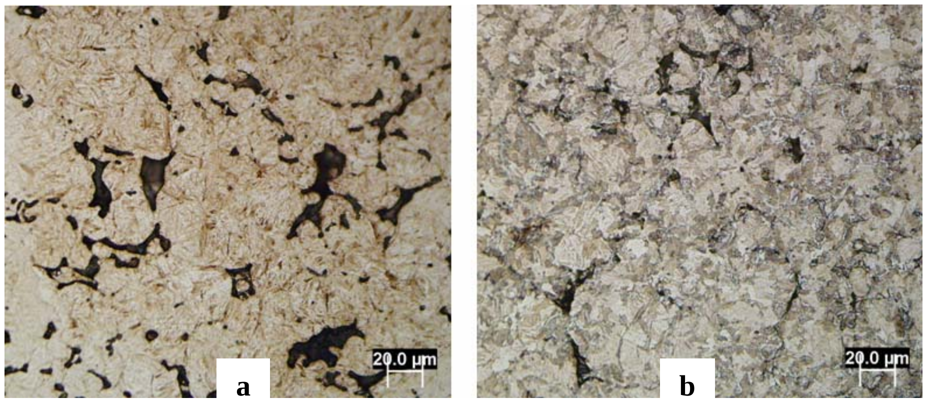

Figure 10. Case hardened Material A: ***a*** – surface area; ***b*** – center area.

Figure 11 shows microstructures of heat treated Material B in nitrogen-hydrogen atmosphere (Figure 11a) and in endogas (Figure 11b).

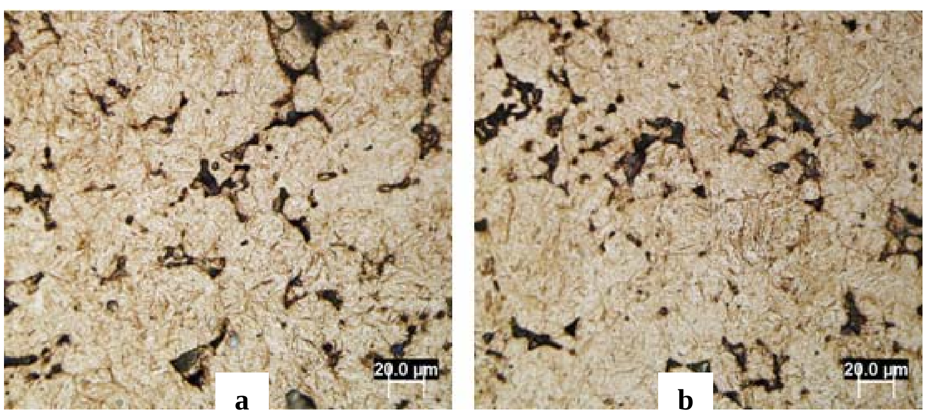

Figure 11. Heat-treated Material B: ***a*** – sintered in nitrogen-hydrogen atmosphere; ***b*** – sintered in endogas

Compared to sintering in nitrogen-hydrogen atmosphere the Material B, previously sintered in endogas, obtained similar martensitic microstructure (Figure 11b).

PROPERTY COMPARISON TO IRON-NICKEL STEEL AND PREALLOYED STEEL

Table VIII shows property comparison of Material B^N – QT (Astaloy CMN, 90 v/o N_2/10 v/o H_2 sintering, through hardened).

Table VIII. Astaloy CMN + 0.6% C comparison to MPIF Standard 35

Material	Fe (%)	C (%)	Ni (%)	Mo (%)	Mn (%)	Cu (%)	Cr (%)
FN-0205-105HT	Bal	0.3 – 0.6	1 – 3	–	–	0 – 2.5	–
FN-0205-130HT	Bal	0.3 – 0.6	1 – 3	–	–	0 – 2.5	–
FN-0405-105HT	Bal	0.3 – 0.6	3 – 5.5	–	–	0 – 2.5	–
FL-4205-100HT	Bal	0.4 – 0.7	0.35 – 0.55	0.5 – 0.85	0.2 – 0.4	–	–
FL-4605-100HT	Bal	0.4 – 0.7	1.7 – 2.0	0.45 – 0.60	0.05 – 0.3	–	–
Astaloy CMN	**Bal**	**0.6**	**0.55**	**0.11**	**0.1**	–	**0.56**

Material	Hardness HRC	TRS MPa (10^3psi)	UTS MPa (10^3psi)	Impact J (ft-lbs)
FN-0205-105HT	29	1110 (160)	720 (105)	6 (4.5)
FN-0205-130HT	33	1310 (190)	900 (130)	8 (6.0)
FN-0405-105HT	25	1000 (145)	720 (105)	7 (5.0)
FL-4205-100HT	32	1100 (160)	690 (100)	9 (7.0)
FL-4605-100HT	29	1140 (165)	690 (100)	8 (6.0)
Astaloy CMN 7.10 g/cm³	**45 - 52**	**>1100 (>160)**	**830 (120)**	**>8 (>6.0)**

As it can be seen the Astaloy CMN is comparable in performance to many of the Iron – Nickel and Prealloyed Steels and shows higher hardness against materials shown in the Table VIII. Astaloy CMN can be economically processed with a combination of density, sintering and heat treated parameters to achieve high performance at a low cost.

CASE STUDY

Gas carburization of spur gears

Many gears require a hard surface and a tough core and these features are commonly achieved by case hardening operations. Based on the results obtained with the test specimens rep case-carburization of spur gear manufactured from Material A was performed. The spur gears, shown in Figure 12, had a diameter Ø31 mm (1.22”), height 15 mm (0.59”) and 18 teeth.

Figure 12. Spur gear used for case carburization study.

The gears were compacted to a green density of 7.20 g/cm^3. Sintering was carried out at 1120°C (2050°F) using the same equipment and conditions as described in Table III. The carburizing was carried out at

Pennsylvania Industrial Heat Treaters in the same equipment used for the test bars with a reduced carburizing time of 15 minutes.

Apparent hardness of 48 HRC was achieved in the surface of the heat treated gears. The microhardness and microstructure obtained in the case and the core of a tooth of a carburized gear is shown in Figure 13.

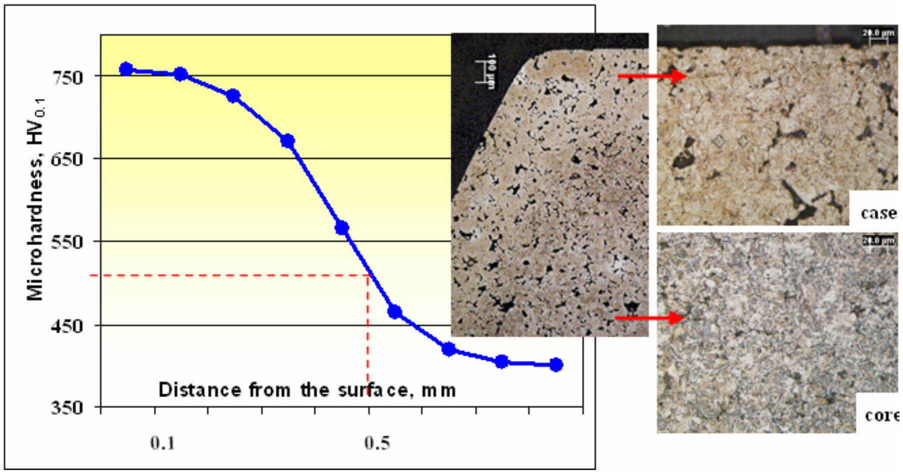

Figure 13. Micro hardness and microstructure of case carburized spur gear.

A micro hardness of 760 $HV_{0.1}$ was achieved in the surface. The microhardness profile measured from the surface and inwards shows a case depth of 0.5 mm had been obtained (515 $HV_{0.1}$ equal to 50 HRC), which is a common case for many gear applications. The microstructure in the case is martensite. In the core a softer mostly bainitic structure was formed.

The result obtained with case carburization on the gears corresponds with the results obtained from the test bars regarding both the microstructure and microhardness profile. The data generated for test bars can therefore be used in the design of components similar to gears. Depending on the component geometry and size the parameters used for carburization should be optimized to obtain the required case depth and microhardness profile.

Through hardening of rings

The evaluation of through hardening based on the results obtained with the test specimens was performed using rings made from material B. The rings, shown in Figure 14, had outer diameter 55 mm (2.165”), inner diameter Ø30 mm (1.181”) and height – 20 mm (0.787”). The rings were compacted to a green density of 7.00 g/cm^3 and sintering at 1120°C (2050°F) using the same equipment and conditions as described in Table III. The heat treatment (quench and temper) was performed in the same equipment used for the test bars and with same conditions as Table IV.

Figure 14. Rings used for through hardening.

Figure 15 shows martensitic microstructure achieved after heat treatment (right image).

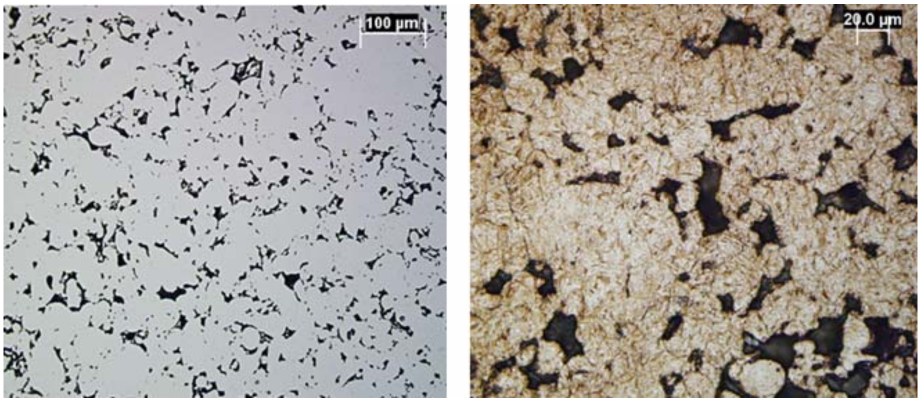

Figure 15. Ring unetched and etched microstructures after through hardening.

Figure 16 shows apparent hardness of heat-treated rings (Material B) sintered in nitrogen-hydrogen atmosphere. Through hardening of rings by quenching and tempering increased the apparent hardness to 45 HRC. This increase is the effect of changing the microstructure from ferrite-pearlite-bainite to martensite in material volume.

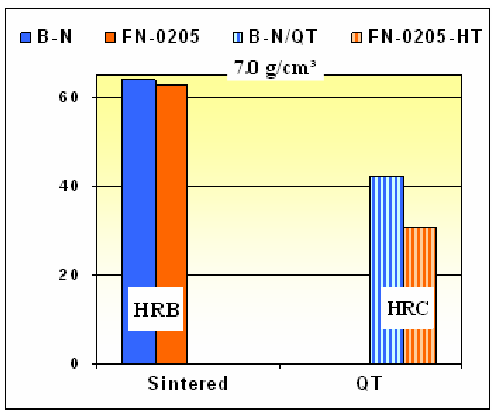

Figure 16. Ring apparent hardness after sintering (left) and through hardening compare to FN-0205.

Table IX shows the data obtained for apparent and micro hardness of heat-treated rings.

Table IX: Through hardened rings

Density		Hardness	M-hardness, case/core
7.0 g/cm³	Ring, B^{N}	64 HRB	-
	Ring, $B^{N/QT}$	44 HRC	802 / 713 $HV_{0.1}$

CONCLUSIONS

Astaloy CMN, a lean pre-alloyed Cr-Ni (with small amount of Mo & Mn), is suitable for different types of heat treatments.

Depending on density, a hardness level up to 50 HRC could be obtained for both materials after heat treatment.

Depending on the processing conditions the transverse rupture strength can be increased up to 40–70%.

Carburization has been demonstrated to be an effective process to case harden spur gears made of Astaloy CMN with carbon content in the range of 0.15 to 0.30 %. The data obtained with test bars and gears corresponds very well. Data determined on the test bars can be used in the design of components that will be carburized.

The carburization of materials based on Astaloy CMN significantly increases the mechanical properties compared to the as sintered material. The properties can be increased by increasing sintering temperature and density.

In a future study, high temperature sintering, vacuum carburizing and heat-treatment will be evaluated as well as distortions and fatigue properties. The carburization with elevated temperature also should be considered. This will decrease partial pressure of oxygen and eliminate the small amount of oxidation.

To ensure future profitability of the whole value chain one key success factor is the availability of cost effective materials. Astaloy CMN offers such a solution.

References

1. S. Berg and B. Maroli. “Properties obtained by chromium-containing material”, *Advances in Powder Metallurgy & Particulate Materials*, compiled by V. Arnhold, C.-L. Chu, W.F. Jandenska, Jr. and H.I. Sanderow, Metal Powder Industries Federation, Princeton, NJ, 2002, part 8, pp.1-14.
2. U. Engstrom, D. Milligan, A. Klekovkin, “Chromium may give pre-alloys the cost edge”, *Metal powder report*, 2006, vol. 61, no. 7, pp. 36-41.
3. Historical data, *http://www.amm.com*